Functionally Graded YSZ/NiCrAlY Coating Prepared by Laser Induction Hybrid Rapid Cladding

Zhou Shengfeng[1] Dai Xiaoqin[2] Xiong Zheng[3] Zhang Tianyou[1]

[1] *School of Material Science and Engineering, Nanchang Hangkong University, Nanchang, Jiangxi* 330063, *China*

[2] *School of Information Engineering, Nanchang Hangkong University, Nanchang, Jiangxi* 330063, *China*

[3] *College of Science, Naval University of Engineering, Wuhan, Hubei* 430074, *China*

Abstract To eliminate cracks and thermally grown oxide (TGO) in thermal barrier coatings (TBCs), the functionally graded yttria-stabilized-zirconia (YSZ)/NiCrAlY coating by laser induction hybrid rapid cladding (LIHRC) is investigated. The results show that the crack-free YSZ/NiCrAlY coating with good profile and gradual microhardness can be obtained when laser scanning speed and powder feeding rate increase to 3200 mm/min and 90.63 g/min during LIHRC, respectively. The c-ZrO_2, m-ZrO_2 and t-ZrO_2 phases in primary YSZ powder are all completely transformed into the metastable t′-ZrO_2 phase. The fine, dense and dual-phase microstructure composed of columnar dendrites is characterized by the gradual increase of YSZ content in the coating. Moreover, the interface of consecutive layer disappears, which is different from ceramic layer-bond layer (i.e., double-layer) constituent of TBCs formed during the individual laser cladding. After the isothermal oxidation, the metastable t′-ZrO_2 phase in the LIHRC-formed functionally graded YSZ/NiCrAlY coating transforms into t-ZrO_2, which can increase the oxidation resistance of superalloy GH4169.

Key words laser technique; laser induction hybrid rapid cladding; functionally graded coating; YSZ/NiCrAlY; microstructure

OCIS codes 140.3390; 350.3850; 350.5030

激光感应复合快速熔覆功能梯度 YSZ/NiCrAlY 涂层的研究

周圣丰[1] 戴晓琴[2] 熊 征[3] 张天佑[1]

[1] 南昌航空大学材料科学与工程学院，江西 南昌 330063

[2] 南昌航空大学信息工程学院，江西 南昌 330063

[3] 中国海军工程大学理学院，湖北 武汉 430074

摘要 为了消除常规热障涂层的裂纹与热生长氧化物(TGO)，研究了激光感应复合快速熔覆制备功能梯度氧化钇稳定的氧化锆(YSZ)和 NiCrAlY 涂层。结果表明，当激光扫描速度与送粉率分别提高到 3200 mm/min 与 90.63 g/min 时，激光感应复合快速熔覆获得的 YSZ/NiCrAlY 梯度涂层经检测无裂纹，具有良好的外形，且显微硬度呈梯度分布。原始粉末内立方氧化锆(c-ZrO_2)、单斜氧化锆(m-ZrO_2)、四方氧化锆(t-ZrO_2)完全转变为亚稳态的四方氧化锆(t′-ZrO_2)。梯度增加 YSZ 的涂层具有组织细小、致密、由柱状树枝晶组成的双相结构特征。此外，连续两层间界面消失，完全不同于单纯激光熔覆获得的陶瓷-粘结层双层结构的热障涂层。等温氧化后，激光感应复合快速熔覆功能梯度 YSZ/NiCrAlY 涂层内亚稳态的四方氧化锆(t′-ZrO_2)转变为稳态的四方氧化锆(t-ZrO_2)，从而提高了高温合金 GH4169 的抗高温氧化性能。

关键词 激光技术；激光感应复合快速熔覆；功能梯度涂层；YSZ/NiCrAlY；显微结构

中图分类号 TG154.5; TN249 **文献标识码** A **doi**: 10.3788/CJL201340.0403004

收稿日期: 2012-10-26; **收到修改稿日期**: 2012-12-07

基金项目: 国家自然科学基金(51261027)资助课题。

作者简介: 周圣丰(1977—)，男，博士，副教授，主要从事激光表面强化与激光快速制造等方面的研究。E-mail: zhousf1228@163.com

1 Introduction

Yttria-stabilized-zirconia (YSZ)-based thermal barrier coatings (TBCs) are widely used for thermal protection of high temperature components in gas turbine and diesel engines for propulsion and power generation due to its low thermal conductivity and high chemical stability[1]. Generally, YSZ-based TBCs are fabricated by plasma spraying and electron-beam physical vapor deposition (EB-PVD). Plasma spraying technique has many advantages such as mature technology, convenient operation and high efficiency. But YSZ-based TBCs produced by plasma spraying have lamellar structure, many porosities and poor bonding to substrate, resulting in an untimely spalling of YSZ-based TBCs in service[2]. Compared with plasma spraying, EB-PVD can fabricate YSZ-based TBCs with a columnar structure and relatively longer life, but has high cost, complex operation and low efficiency[3]. The constituent of YSZ-based TBCs is composed of superalloy bond layer and ceramic YSZ layer. This double-layer constituent of TBCs often induces the formation of thermally grown oxide (TGO) in the interface of bond layer and ceramic layer under high temperature, resulting in the failure of TBCs[4]. Moreover, the ceramic YSZ layer easily suffers from the spalling during thermal cycling due to their significantly different physical properties of the bond layer and the ceramic layer in the interface[5].

Being different from the common methods for producing TBCs like plasma spraying and EB-PVD, laser cladding can especially produce TBCs with fine microstructure, low dilution and high bonding to substrate[6]. However, the common problems for laser cladding such as cracks and low cladding efficiency hinder FG-TBCs from wide application in industry[7~9]. Additionally, TBCs produced by laser cladding are easy to form a ceramic layer-bond layer (i.e., double-layer) constituent. This double-layer constituent can induce the ceramic YSZ layer to crack during thermal cycling[10]. The main reason is that the density of NiCrAlY is much higher than that of YSZ particles and that the violent stirring and convection are driven by thermocapillarity[11]. The ceramic YSZ layer susceptibly grows at the top of coatings while the bond NiCrAlY layer is formed at the bottom of coatings, which induces to form the residual stress during rapid solidification. If the residual stress is higher than the strength of coating, crack originates and propagates in the coating.

To eliminate cracks of cladding layer and increase cladding efficiency, laser induction hybrid rapid cladding (LIHRC) has been put forward and well developed[12]. Moreover, the high laser scanning speed can also reduce the time of the convection and stirring in the molten pool during LIHRC[13], which can help YSZ particles to distribute homogeneously in TBCs. Accordingly, the double-layer constituent formed during the individual laser cladding can be eliminated during LIHRC. In recent years, the functionally graded TBCs (i.e., FG-TBCs) have also been investigated due to their many unique characteristics such as the gradual change in composition, microstructures and properties, which can reduce the microstructure stress and improve the crack sensitivity of TBCs[14]. Moreover, compared with the common double-layer constituent of TBCs, FG-TBCs can eliminate the interface of ceramic layer-bond layer and the formation of TGO to increase the lifetime of TBCs. Therefore, FG-TBCs have attracted significant attention in recent years. However, FG-TBCs prepared by LIHRC have not been reported. The emphasis of this paper is to characterize the functionally graded YSZ/NiCrAlY coating prepared by LIHRC on superalloy GH4169.

2 Experiment

The ceramic powder is 8% (mass fraction) YSZ, whose size is in the range of 30 ~ 65 μm. The bond powder used is NiCrAlY superalloy ($Ni_{20}Cr_8Al_{0.4}Y$) with a grain distribution of 40 ~ 70 μm, whose chemical composition is listed in Table 1. The superalloy GH4169 with a dimension of 100 mm × 40 mm × 4 mm is used as the substrate, whose chemical composition is also listed in Table 1. The functionally graded YSZ/NiCrAlY coating by LIHRC consisted of six cladding layers, where the contents (mass fraction) of ceramic YSZ are 0%, 2%, 6%, 10%, 14% and 18%, respectively.

Table 1 Chemical composition of bond powder and substrate (mass fraction, %)

Material	C	Cr	Al	Y	Ni	Si	Mn	Mo	Nb	Ti	Fe
Bond powder	0	20	8	0.4	Bal.	0	0	0	0	0	0
Substrate	0.03	19.0	0.57	0	52.3	0.05	0.03	3.06	5.07	1.00	Bal.

The apparatus of LIHRC has been described in detail in our previous paper[11]. The following parameters of laser induction hybrid processing are adopted. Laser power used is 5 kW and scanning speed is 1000～3500 mm/min. The power of induction heater is 30～80 kW and the operation frequency is 50 kHz. The preheated average temperature of substrate is varied from 973 to 1223 K by adjusting the power of induction heater. The powder feeding rate is varied from 20 to 150 g/min. The coating with large area is prepared by multi-track overlapping LIHRC and the overlapping rate is 50%. The height of single cladding layer produced by LIHRC was in the range of 0.4～0.6 mm. Argon gas is used to minimize the surface contamination of coating.

The coatings are separated from the substrate by electric spark computer numerically controlled (CNC) wire-cut machine to carry out the experiment of oxidation resistance. An isothermal oxidation is carried out in a tube furnace with a static atmosphere and maximum operation temperature of 1573 K. Oxidation tests are performed at 1273 K for 100 h. The weight change of oxidized samples is continuously measured by an electronic balance with an accuracy of 0.1 mg after a chosen time of 10 h and air-cooled to room temperature. X-ray diffraction (XRD) analysis is also employed to characterize the formed oxide.

The specimens are also detected by dye penetrant non-destructive testing (DPNDT) to show the presence of porosity and cracks, and then cut, polished carefully and etched by 10% HNO_3 + C_2H_5OH (volume fraction) solution to reveal the microstructure, which is examined in detail by using the optical microscope and scanning electron microscope (SEM). XRD analysis is performed by means of D8ADVANCE diffractometer in Bragg-Brentano configuration to analyze the quantitative phases in the coating (target: Cu, 40 kV, 30 mA). The microhardness measurement is performed by a Vickers-1000 microhardness tester with a load of 1.96 N and a dwelling time of 20 s.

3 Results and discussion

To obtain the coating with low dilution and good profile without cracks and porosity, the optimized parameters are adopted as follows: 5 kW laser power, 3200 mm/min scanning speed, 4 mm spot diameter, 90.63 g/min powder feeding rate, 1173 K preheating temperature, and 53° injection angle of powder nozzle with the surface of substrate. The multi-track overlapping functionally graded YSZ/NiCrAlY coating with a height of 3.2 mm has a relatively smooth surface and good profile without cracks on superalloy GH4149, as shown in Fig. 1.

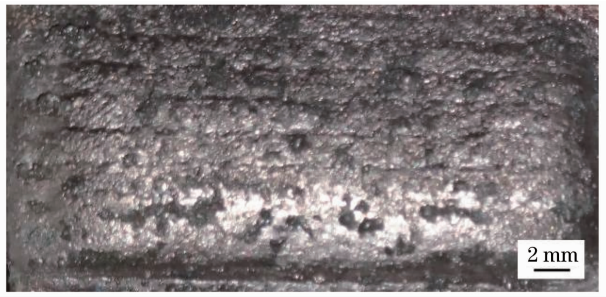

Fig. 1 Surfacemorphology of functionally graded YSZ/NiCrAlY coating on GH4169.

Figure 2 shows the typical cross-section of multi-track overlapping functionally graded YSZ/NiCrAlY coating. It can be seen from Fig. 2(a) that the coating takes on a planar growth in the interface of coating-substrate, followed by a thin cellular structure with a thickness of 1 ～ 2 μm and the columnar dendrites perpendicular to the surface of substrate. It is explained by the following reasons. When the rapid solidification starts by expitaxial growth from the molten NiCrAlY bond, a constitutional undercooling is soon generated in the interface of coating-substrate. As a result, the planar solid-liquid interface becomes unstable, leading to an initiation of columnar dendrite. The formation of columnar dendrites can promote the absorption of thermal strains and effectively deflect the transverse cracks to hinder the propagation of cracks[6]. So the porosity and cracks detected by DPNDT are not found in the coating.

As shown in Fig. 2(b), the interface of consecutive layer in functionally graded YSZ/NiCrAlY coating disappears. It is explained by the following reasons. The previous layer is slightly remelted by heating source of LIHRC. The solidification of the next layer is initiated by epitaxial growth. Obviously, the nucleation has not occurred, but the crystallographic orientation and the structure of the previous layer are reproduced during LIHRC [Fig. 2(c)]. It is noted that the bond NiCrAlY and ceramic YSZ particles are completely melted and solidify to form a fine, dense and dual-phase microstructure during LIHRC. However, YSZ-based TBCs by the individual laser cladding are susceptible to

cracks in the near-interface zones of bond layer and YSZ layer, leading to the spallation of coating[15]. Compared with the common double-layer constituent of YSZ-based TBCs by the individual laser cladding, the functionally graded constituent can eliminate the fragile interface to form the crack-free YSZ/NiCrAlY coating by LIHRC.

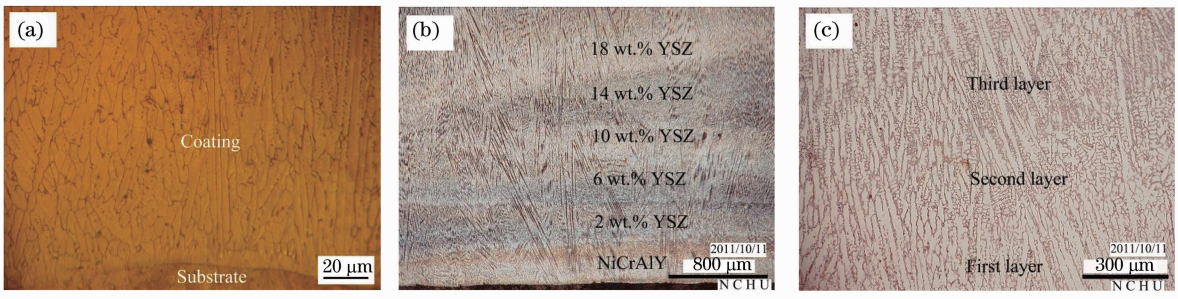

Fig. 2　Morphology of functionally graded YSZ/NiCrAlY coating (a), (b) in the interface of coating-substrate and (c) in the interface of consecutive layer.

The XRD profiles of primary YSZ powder and coating are shown in Fig. 3. The cubic ZrO_2 (c-ZrO_2) and monoclinic ZrO_2 (m-ZrO_2) predominate in the low 2θ range (i.e., 27°～45°), where the tetragonal ZrO_2 (t-ZrO_2) has a low intensity. Furthermore, the cubic ZrO_2 with (331) and (420) peaks is detected, but m- and t-ZrO_2 phases are not found in a relatively higher 2θ range [Fig. 3(b)]. The semi-quantitative analysis of the primary YSZ powder by XRD shown in Table 2 indicates that the primary YSZ powder is composed of c-ZrO_2 (58%, mass fraction), m-ZrO_2 (36%) and t-ZrO_2 (6%). After LIHRC, the XRD result of functionally graded YSZ/NiCrAlY coating is shown in Fig. 3(c). It can be seen that the coating consists of γ-Ni with a face-centered cubic (FCC) structure and t′-ZrO_2 with a non-transformable tetragonal structure. Their contents in the coating are 82% and 18% (Table 2), respectively. The ceramic YSZ particles can be completely melted into liquid due to their high electrical resistivity, and then martensitic-like transformation occurs during LIHRC[7]. Namely, c-ZrO_2 in the primary YSZ powder is melted during LIHRC, and then transforms into the metastable t′-ZrO_2 by a diffusionless and displacive mechanism, not transforming into monoclinic ZrO_2.

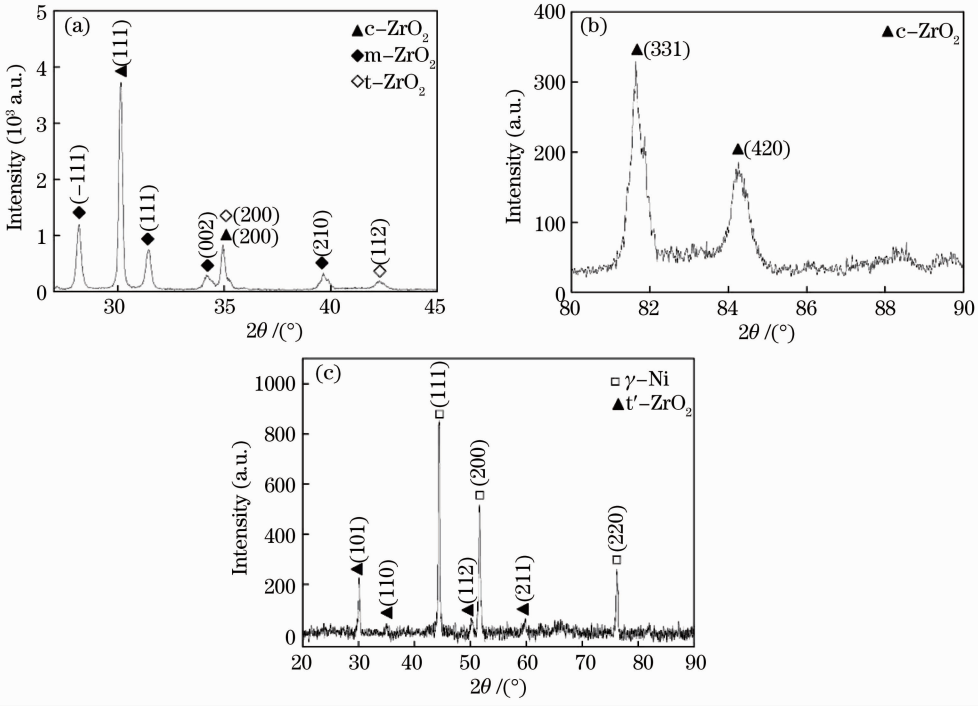

Fig. 3　XRD profiles of primary YSZ powder and functionally graded YSZ/NiCrAlY coating. (a), (b) Primary YSZ powder; (c) functionally graded YSZ/NiCrAlY coating.

Table 2 Phase contents in the primary powder and functionally graded coating (mass fraction, %)

Material	c	m	t	t′	γ
Primary powder	58	36	6	0	0
Functionally graded coating	0	0	0	18	82

The previous result shows that the delamination phenomenon and the interface of ceramic layer-bond layer can be clearly observed in the individual laser cladding coating due to low laser scanning speed and large density difference between ceramic YSZ and bond Ni-based alloy[15]. So it is very difficult to produce the functionally graded YSZ/NiCrAlY coating by the individual laser cladding. However, the time of the stirring and convection in the molten pool can be significantly decreased due to very high laser scanning speed (i.e., 3200 mm/min) during LIHRC. The stirring and convection have no enough time to contribute YSZ particles to float upward in the molten pool. Therefore, the peaks corresponding to γ-Ni and t′-ZrO_2 can be detected simultaneously in the coating [Fig.3(c)], showing that the coating has a mixed and dense microstructure and is only composed of γ-Ni and t′-ZrO_2 (Fig.2).

Figure 4 shows the microhardness profiles of substrate (SUB), heat-affected-zone (HAZ) and every cladding layer. The results indicate that the microhardness of coating presents a graded distribution and increases with an increase in cladding layer. For a single cladding layer, the distribution of microhardness has a homogeneous characteristic. The top layer (i.e., the sixth layer) has the highest microhardness, whose average value is approximately up to 1136 $HV_{0.2}$. As mentioned above, the content of ceramic YSZ increases with cladding layer. The different crystal structures such as c-ZrO_2, m-ZrO_2 and t-ZrO_2 in the primary YSZ powder completely transform into the metastable t′-ZrO_2 accompanying with the molten NiCrAlY. The dual-phase and dense microstructure is formed and the metallic bond γ-Ni is reinforced accordingly. Moreover, the microstructure is composed of fine columnar dendrites and similar in all cladding layers due to rapid heating and rapid solidification during LIHRC. The fine and dual-phase microstructure can not only increase the microhardness of coating, but also improve the toughness of coating[16]. Therefore, the crack-free YSZ/NiCrAlY coating with high and gradual microhardness can be obtained by LIHRC.

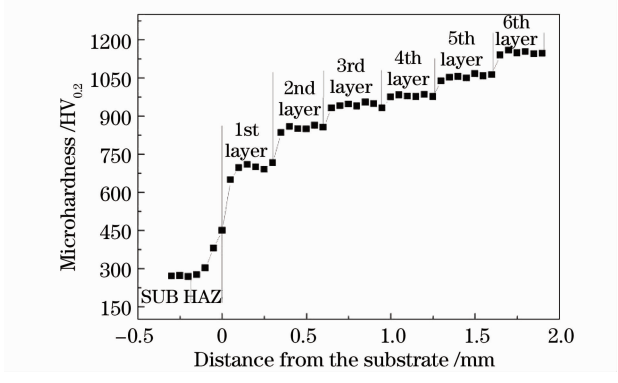

Fig.4 Microhardness of functionally graded YSZ/NiCrAlY coating.

Figure 5 shows the oxidation kinetics of coating and superalloy GH4169. It can be seen that the weight gain of superalloy GH4169 is higher than that of NiCrAlY coating and functionally graded YSZ/NiCrAlY coating by LIHRC. The rate of weight gain for superalloy GH4169 is approximately reduced by 40% when NiCrAlY coating is produced by LIHRC. The Al_2O_3 and $NiCr_2O_4$ oxides are formed on the surface of NiCrAlY coating after isothermal oxidation [Fig.6(a)]. However, the weight gain for superalloy GH4169 can be further decreased by 62% when the functionally graded YSZ/NiCrAlY coating is produced by LIHRC. The oxides such as t-ZrO_2, Al_2O_3 and $NiCr_2O_4$ are formed on the surface of functionally graded YSZ/NiCrAlY coating after isothermal oxidation [Fig.6(b)]. It indicates that the functionally graded YSZ/NiCrAlY coating by LIHRC can markedly increase the oxidation resistance of superalloy GH4169 during isothermal oxidation.

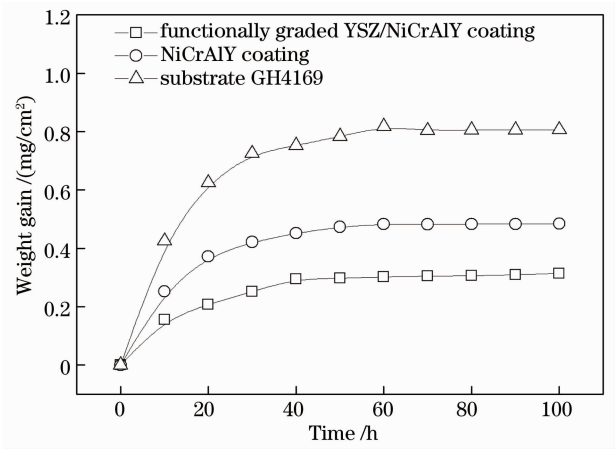

Fig.5 Oxidation kinetics of coating and substrate at 1273 K.

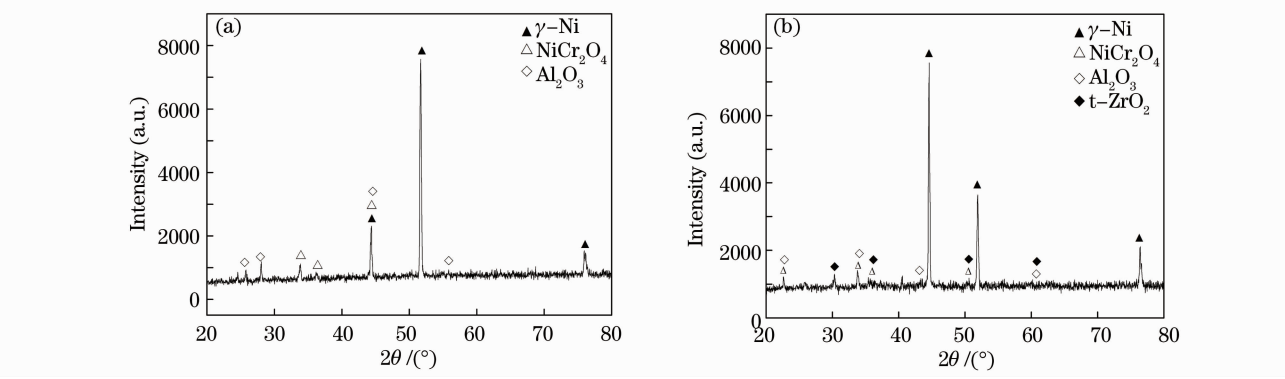

Fig. 6 XRD profiles ofcoatings after isothermal oxidation at 1273 K for 100 h. (a) NiCrAlY coating; (b) YSZ/NiCrAlY coating

4 Conclusions

Thecrack-free YSZ/NiCrAlY coating with good profile and gradual microhardness can be obtained when the laser scanning speed and the powder feeding rate are 3200 mm/min and 90.63 g/min during LIHRC, respectively. The different crystal structures such as c-ZrO_2, m-ZrO_2 and t-ZrO_2 in the primary YSZ powder completely transform into t′-ZrO_2. The fine and dense microstructure presents a characteristic of the columnar dendrites and is composed of dual phase γ-Ni and t′-ZrO_2. Moreover, the interface of consecutive layer in the functionally graded YSZ/NiCrAlY coating by LIHRC also disappears, which is different from the double-layer constituent (i.e., ceramic YSZ layer-bond layer) by the individual laser cladding. After the isothermal oxidation, the metastable t′-ZrO_2 phase in the LIHRC-formed functionally graded YSZ/NiCrAlY coating transforms into t-ZrO_2, which can increase the oxidation resistance of superalloy GH4149.

References

1 L. Yong, J. L. Chang, Z. Qiang *et al*.. Influence of TGO composition on the thermal shock lifetime of thermal barrier coatings with cold-sprayed MCrAlY bond coat [J]. *J. Thermal Spray Tehchnol.*, 2010, **19**(1-2): 168～177

2 C. Pan, X. Xu. Microstructural characteristics in plasma sprayed functionally graded ZrO_2/NiCrAlT coatings [J]. *Surf. Coat. Technol.*, 2003, **162**(2-3): 194～201

3 D. L. Youchison, M. A. Gallis, R. E. Nygren *et al*.. Effects of ion beam assisted deposition, beam sharing and pivoting in EB-PVD processing of graded thermal barrier coatings [J]. *Surf. Coat. Technol.*, 2004, **177-178**(30): 158～164

4 S. Rangaraj, K. Kokini. Interface thermal fracture in functionally graded zirconia-mullite-bond coat alloy thermal barrier coatings [J]. *Acta Materialia*, 2003, **51**(1): 251～267

5 B. C. Wu, E. Chang, C. H. Chao. The oxide pegging spalling mechanism and spalling modes of ZrO_2 8wt%-Y_2O_3/Ni-22Cr-10Al-1Y thermal barrier coatings under various operating-conditions [J]. *J. Mater. Sci.*, 1990, **25**(2): 1112～1119

6 V. K. Balla, P. P. Bandyopadhyay, S. Bose *et al*.. Compositionally graded yttria-stabilized zirconia coating on stainless steel using laser engineered net shaping (LENS™) [J]. *Scripta Materialia*, 2001, **57**(9): 861～864

7 J. H. Ouyang, S. Nowotny, A. Richter *et al*.. Characterization of laser clad yttria partially-stablized ZrO_2 ceramic layers on steel 16MnCr5 [J]. *Surf. Coat. Technol.*, 2001, **137**(1): 12～20

8 Wang Dongsheng, Tian Zongjun, Wang Jingwen *et al*.. A method of crack control in laser cladding process with changing power density distribution of laser beam [J]. *Chinese J. Lasers*, 2011, **38**(1): 0103004
王东生, 田宗军, 王泾文 等. 一种通过改变激光功率密度分布控制熔覆层裂纹的方法 [J]. 中国激光, 2011, **38**(1): 0103004

9 Gao Xuesong, Tian Zongjun, Shen Lida *et al*.. Study on Al_2O_3-13% TiO_2 coatings prepared by laser cladding and thermal shock resistance [J]. *Chinese J. Lasers*, 2012, **39**(2): 0203006
高雪松, 田宗军, 沈理达 等. 激光熔覆 Al_2O_3-13% TiO_2 陶瓷层制备及其抗热震性能 [J]. 中国激光, 2012, **39**(2): 0203006

10 Y. T. Pei, J. H. Ouyang, T. C. Lei *et al*.. Laser clad ZrO_2-Y_2O_3 ceramic/Ni-base alloy composite coatings [J]. *Ceramic International*, 1995, **21**(2): 131～136

11 P. A. Carvalho, R. Vilar. Laser alloying of zinc with aluminum: solidification structures [J]. *Surf. Coat. Technol.*, 1997, **91**(3): 158～166

12 S. Zhou, Y. Huang, X. Zeng *et al*.. Microstructure characteristics of Ni-based WC composite coatings by laser induction hybrid rapid cladding [J]. *Mater. Sci. Eng. A*, 2008, **480**(1-2): 564～572

13 S. Zhou, X. Zeng, Q. Hu *et al*.. Analysis of crack behavior for Ni-based WC composite coatings by laser induction hybrid rapid cladding [J]. *Appl. Surf. Sci.*, 2008, **255**(5): 1646～1653

14 A. Rabiei, A. G. Evans. Failure mechanisms associated with thermally grown oxide in plasma-sprayed thermal barrier coating [J]. *Acta Materialia*, 2000, **48**(15): 3963～3976

15 Y. T. Pei, J. H. Ouyang, T. C. Lei. Laser cladding of ZrO_2-(Ni alloy) composite coating [J]. *Surf. Coat. Technol.*, 1996, **81**(2-3): 131～135

16 M. Es-Souni, R. Wagner, P. A. Beaven. Microstructure and phase relationships in a rapid solidified dual phase alloy on Ti_3(Al, Si)+Ti_5(Si, Al)$_3$[J]. *Mater. Sci. Eng. A*, 1992, **151**(1): 69～75

栏目编辑: 宋梅梅